IARJSET
ISSN (Online) 2393-8021
ISSN (Print) 2394-1588
International Advanced Research Journal in Science, Engineering and Technology
ISO 3297:2007 Certified
Vol. 3, Issue 9, September 2016

Design &Analysis of Perforated Rectangular Fin Array with Varying Percentage of Perforation

Mitesh H. Patil[1], Santosh V. Patil[2], Dr. E. R. Deore[3], Gaurav A. Chaudhari[4]

PG Student, Mechanical Department, SSVPSCOE, Dhule, Maharashtra, India[1]

Asst. Professor, Mechanical Department, SSVPSCOE, Dhule, Maharashtra, India[2]

H.O.D, Mechanical Department, SSVPSCOE, Dhule, Maharashtra, India[3]

M.E. Heat Power[4]

Abstract: The present experimental study focus on the design and analysis of perforated rectangular fin array with varying percentage of perforation. Recently the fins are commonly used to increase the heat transfer rate between the surrounding fluid and surfaces in heat exchange appliances. Various fin geometries available with different shape, size and perforation, in this experiment we use the rectangular fins having different percentage of perforation such that plane, 10%, 20% and 30% of perforation. The effects of perforations and base-to-ambient temperature difference on the heat transfer performance of fin arrays were observed and optimum value of perforation is suggested. The experimental set-up was employed during experiments in order to take measurements from 4 different fin configurations having fin lengths of 180 mm and fin height of 20 mm. Fin spacing was maintained fixed at 7.45 mm. Fin thickness is 3 mm. 5 heat inputs ranging from 25 W to 67.5 W were supplied for all fin configurations, and hence, the base and the ambient temperatures were measured in order to evaluate the heat transfer rate from fin arrays. The CFD analysis can be done by using above parameters and fin configuration. The results of experimental as well as CFD analysis have shown that the convection heat transfer rate from fin arrays depends on all percentage of perforation and base-to-ambient temperature difference. Analysis gives the idea about heat transfer and behaviour of perforated fins. The effect of flow visualization also cleared the heat transfer by chimney flow pattern. From above analysis we get 30% perforation gives more heat transfer than other perforation.

Keywords: Perforation, Fins, Steady state, Natural convection, CFD

1. INTRODUCTION

Currently, the so many industries are suffering from the problem of overheating which causes due to heat generation in the appliances. The industries manufacture the appliances with compact size with low cost. Therefore appliance with compact size and other appliances also generate the heat in system due to so many reason and causes overheating problem. This produced heat which damage the system due to overheating. This engendered heat in a system should be dissipated in the surrounding so as to retain the system at its endorsed working temperatures. Therefore, devising efficient cooling solutions to meet these tasks is of paramount importance and has direct effects on the reliability and performance of electronic devices and power electronic devices. Therefore to overcome the problem of overheating in thermal system. Thermal systems using adequate emitters as fins are necessary. If we want to attain the required heat transfer rate, with the smallest quantity of material, the preparation of geometry & positioning of the fins should be optimal. Between these variations of geometry, fins have rectangular shape are the most commonly used fin geometry for the reason that their simple structure, low manufacture cost and high thermal efficiency.

There are two types of alignments with affections to quadrilateral fin arrangements, vertically based vertical fins and horizontally based vertical fins, have been more commonly used in the devices. However, the horizontal alignment isn't better because of its moderately inferior capacity to disintegrate heat. The simple equation of convection heat losses is given by:

$$Q_c = h \times A \times \Delta T \qquad (1)$$

From equation 1, we can increase the heat transfer rate either by increasing the surface area of fin A, or by increasing heat dissipation coefficient h. The value of heat transfer coefficient h can be enhanced by using proper condition of forced flow over the essential surface. While the forced convection is effective. It needs an extra space for the fan or blower which interns causes the enhancement in initial and maintenance cost. Hence forced convection isn't always selectable. For increasing the heat transfer rate, it is poorer, suitable and easy to use the extended surfaces.

To increase the heat transfer area, it is very effective to use the fins over the surface. Therefore the result of heat transfer will be improved. However, if the no. of fins and the spacing between two fins aren't appropriately designed then the heat transfer rate can be decrease also. Though adding extra number of fins increases flow of air and

IARJSET
ISSN (Online) 2393-8021
ISSN (Print) 2394-1588
International Advanced Research Journal in Science, Engineering and Technology
ISO 3297:2007 Certified
Vol. 3, Issue 9, September 2016

cause the boundary layer disruptions which upset the heat transfer indifferently. The investigational judgments allied to the thermal performances of fins with rectangular shape were testifying in literature. In this study, the steady state condition of natural convection heat exchange as of perforated vertical fin with rectangular shape conformation protruding from a vertical base will be studied.

2. DESIGN AND EXPERIMENTAL SETUP

2.1 Design and Finalization of Fin Geometry

Base temperature = T_s = 60℃ to 115℃

Ambient temperature = T_∞= 30℃

Film temperature $T_f = \frac{T_s + T_\infty}{2} = 45℃ \text{to } 72.5℃$

$$R_a = \frac{g\beta\Delta T L_c^3}{\nu^2} \times P_r = 1.0396 \times 10^7 \text{ to } 1.5985 \times 10^7$$

$$S_{opt} = 2.714 \times \left(\frac{L}{R_a^{0.25}}\right) = 8 \text{ mm}$$

Assume fin height H = 20mm

Material - Aluminum

t = 3mm,

ρ=2700 Kg/m3,

C_p=0.903 $^{KJ}/_{Kg}$

Volume V = {(180 x 120 x 5) + [(180 x 20 x 3) x 11]}
= 226800 mm3
= 2.268 x 10^{-4} m3

Mass, M = ρ x V = 2700 x 2.268 x 10^{-4}= 0.610 kg

Heat Capacity = M×C_p = 0.5508 $^{KJ}/_{K}$

$$\text{No. of fins} = \frac{\text{Length of base plate}}{S + t} = \frac{120}{8 + 3} = 11 \text{ fins}$$

Table.1 Dimensions of Fin Configuration

Fin Spacing (s) Mm	Fin Height (H) Mm	Base Thickness (d) Mm	Fin Width (W) Mm	Fin length (L) Mm
8	20	5	120	180
Material	Set ID		Fin Thickness (t) mm	Number of Fins (n)
Aluminum	Plane Fin Array		3	11
Aluminum	10% perforation		3	11
Aluminum	20% perforation		3	11
Aluminum	30% perforation		3	11

2.2 Test Procedure

In order to be able to determine the convective heat transfer performances of the fin arrays under steady-state conditions, total heat losses from the set-ups should be calculated first. Hence, the experimental set-ups will be calibrated and the calibration method will be verified before starting experiments. The total heat, which occurs as a result of the power inputs to the heaters, is dissipated in modes of natural convection, radiation from the fin arrays and conduction from the remaining parts of the set-ups. Since the heat transfer coefficients cannot be determined by the current experimental method, direct estimation of the convection heat transfer rates from the fin arrays is proposed in this experimental set up.

2.3 Calibration of Setup

For the calibration of the set-ups, the heat transfer rate from the heated base-plate should be determined. Since the experimental set-ups had similar properties except dimensions, the solution procedures of heat conduction equations were same. The heat conduction equation was solved with the method of integral transform technique. For the heat transfer rate from heated base-plate, the following equation is obtained:

$$\frac{\dot{Q}_{out}}{\dot{Q}} = \zeta - \tau \frac{T_w - T_a}{\dot{Q}} \qquad (1)$$

where $\dot{Q}$ is the power input to the heater, Ta is the ambient temperature, Tw is the average surface temperature of the heated plate, $\dot{Q}_{out}$ is the total heat transfer rate from the heated plate and, ζ and τ (W/K) are constants that depend on the geometry and the average thermal conductivity of the system. The constants (ζ, τ) of the calibration equation can be found if and only if the total heat transfer rates are known. Since the parameters ($\dot{Q}$, Ta and Tw) in Eq. (1) can be measured, the rate of heat transfer through the heated plate should be calculated with these data set. Moreover, the total heat transfer rate should not involve the convective component since the heat transfer coefficients cannot be estimated directly. For this reason, two parallel plates will be attached opposite to each other and were mounted onto the each set-up as shown in Figure 1. These plates will be of the same size and same material as the base-plates of fin arrays. The calibration plate dimensions will be decided on the dimensions of test setup. For each of the set-ups, the distance between the plates will be kept fixed at 1.8 mm by means of four fiber supports at the corners of the plate to create conditions to prevent the convection heat transfer.

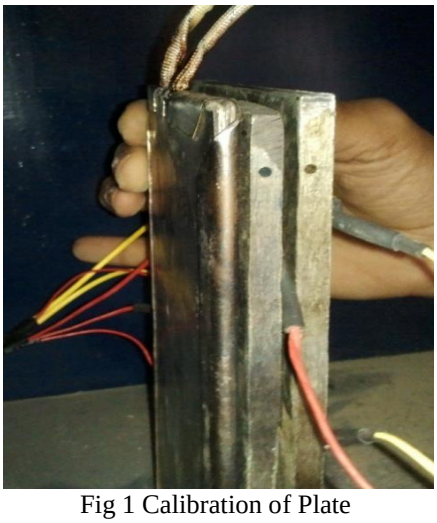

Fig 1 Calibration of Plate

IARJSET
ISSN (Online) 2393-8021
ISSN (Print) 2394-1588
International Advanced Research Journal in Science, Engineering and Technology
ISO 3297:2007 Certified
Vol. 3, Issue 9, September 2016

In order to have pure conduction through the air between the plates, either the Rayleigh number based on plate length (180 mm) had to be less than 1000, or the aspect ratio (ratio of the plate length to the distance between the plates) had to be greater than or equal to 100. Since the Rayleigh number based on plate length is of the order of 10^6, the first criterion could not be achieved with air. However, the second criterion will be satisfied for calibration plates since the ratios are greater than 100. Therefore, the heat transfer between the plates was by conduction and radiation. At steady state, the heat transfer between the plates will have the following form:

$$\dot{Q}_{out} = \frac{k}{d} A (T_1 - T_2) + \sigma \left(\frac{\varepsilon}{2-\varepsilon}\right) A \left(T_1^4 - T_2^4\right) \quad (2)$$

In Eq. (2), k is the thermal conductivity of air between the plates, will be evaluated at the average of plate temperatures, T1 is the temperature of heated plate, T2 is the temperature of opposite plate, d is the distance between the plates, σ is the Stefan-Boltzmann constant and ε is the emissivity of the plates, assumed as 0.20. This value agreed well with those given in literature.

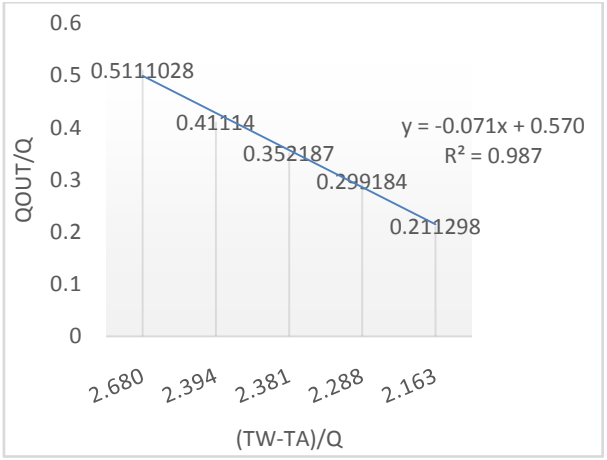

Figure 2 Calibration Curve for Set-up

Using these plots, ζ and τ (W/K) values were determined and calibration equations were obtained as

$$\frac{\dot{Q}_{out}}{\dot{Q}} = 0.5705 - 0.0712 \frac{T_w - T_a}{\dot{Q}} \quad (3)$$

The value of ζ, 0.5705 is dimensionless and the coefficient of (Tw-Ta)/Q term, 0.0712 have the dimension of (W/K).

2.4 Verification of Calibration Method

In order to determine the validity of the used calibration equations and method, a set of experiments will be conducted on a vertical plate for each set-up. Using the experimental results, experimentally and theoretically estimated Nusselt numbers were will be compared for verification. For each of the set-ups, predetermined power inputs will be supplied to heat the vertical plates. Under steady-state conditions, the vertical plate temperatures, Tw, the ambient temperatures, Ta and the power inputs, will be measured. For each power input, the total heat transfer rate from vertical plate will be calculated by substituting the measured data into Eq. (2). Then, the radiation heat transfer rate from vertical plate was estimated by assuming the environment as a blackbody at ambient temperature Ta as:

$$(\dot{Q}_o)_r = \sigma \varepsilon A \left(T_w^4 - T_a^4\right) \quad (4)$$

The convection heat trans0fer will be calculated for vertical plate as

$$(\dot{Q}_o)_c = \dot{Q}_o - (\dot{Q}_o)_r \quad (5)$$

Therefore heat transfer coefficient based on the surface area of the vertical plate will be calculated as

$$h = \frac{(\dot{Q}_o)_c}{A \,.\, (T_w - T_a)} \quad (6)$$

Rayleigh number and Nussult number will be then evaluated as

$$R_a = \frac{g\beta\Delta T L^3 (T_w - T_a)}{\nu \alpha} \quad (7)$$

$$N_{u\,exp.} = \frac{h_{exp.}\ L}{k} \quad (8)$$

Where L, is the length of the vertical plate is the characteristic length. The thermo-physical properties necessary to evaluate Rayleigh and Nusselt numbers will be taken at the film temperature $T_f = (T_w + T_a)/2$.

After determining experimental Nusselt numbers for both of the set-ups, they will be compared with the Nusselt numbers evaluated by using available vertical plate correlations from literature.

The correlations which will be utilized for the comparison are:

1.Churchill and Chu's first relation (for laminar and turbulent flows):

$$N_{u\,th} = \left\{ 0.825 + \frac{0.387 \,.\, (R_a)^{\frac{1}{6}}}{\left[1 + \left(\frac{0.492}{Pr}\right)^{\frac{9}{16}}\right]^{\frac{8}{27}}} \right\}^2 \quad \text{for } 10^{-1} < R_a < 10^{12} \quad (9)$$

2. Churchill and Chu's second relation (for laminar flows only):

$$N_{u\,th} = 0.68 + \frac{0.67 \,.\, (R_a)^{\frac{1}{4}}}{\left[1 + \left(\frac{0.492}{Pr}\right)^{\frac{9}{16}}\right]^{\frac{4}{9}}} \quad \text{for } 10^{-1} < R_a < 10^{9} \quad (10)$$

3. Mc. Adams Relation :

$$N_{u\,th} = 0.59 \,.(R_a)^{1/4} \quad (11)$$

The theoretical and experimental Nusselt numbers will be then plotted in the same graph in order to display the agreement between them. Also the percentage relative

IARJSET
ISSN (Online) 2393-8021
ISSN (Print) 2394-1588
International Advanced Research Journal in Science, Engineering and Technology
ISO 3297:2007 Certified
Vol. 3, Issue 9, September 2016

errors of these correlations with respect to the Nusselt numbers will be evaluated from the experimental data.

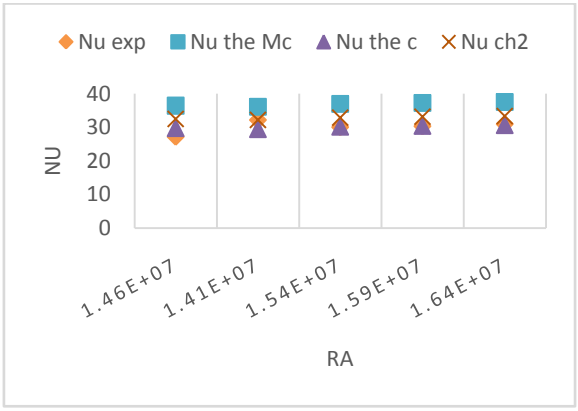

Fig. 3 Comparison of Experimental and Theoretical Nusselt Numbers

Examination of Figure reveals that the experimental data are in a good agreement with the correlations. The average relative errors are less than 20 % for Churchill and Chu's and McAdams' correlations. These results indicate the validity of the experimental set-ups, the experimental procedure and the calibration method.

2.5 Testing Procedure of Fin Array

The experimental set-up will consists of an aerated concrete case and supporting frame on which the concrete is mounted, and various instruments for measuring the ambient temperature, base-plate temperature and the power input for the heater. The essential dimensions of the components of Set-up will be as given in Table.1. The frames of set-up will be filled with Heatlon in order to maintain the insulation of the aerated concrete cases. The front surfaces of the frames will be covered with metal plates, which have rectangular holes at the center, so that fin arrays are placed into the cases through these holes.

The heaters will be placed into these cases. 3 mm thick aluminum plates will be located between the heaters and base-plates in order to distribute the power input evenly. Thus, a more uniform temperature distribution at the base of the fin array can be achieved. Each heater covered by cases will fully consists of a nichrome wire wound around a thin mica plate and mica sheets on both sides of mica plate for insulation. They will be selected as 600 W and 220 V, AC The test sections will be insulated carefully.

The aerated concrete case insulating the rear surface of the heater and the four lateral surfaces of the fin base-plate will be used as the primary insulation material. The remaining part between set-up boundaries and concrete will be filled with heatlon serving as the secondary insulation. Therefore, the boundaries of the set-ups will be maintained approximately at the ambient air temperature. The case material will be chosen as aerated concrete due to its high insulation quality (thermal conductivity, k ~ 0.15 W/m K) and high temperature resistance.

Figure 4 Experimental setup

In addition, it can be shaped easily so that all necessary processes, digging, drilling etc., can be performed on these materials. The experiments will be then conducted in a windowless large room. Precautions will be taken to maintain almost constant room temperature and free of air currents.

The fin configurations will be produced by milling longitudinal grooves in one of the faces of a rectangular bar. The fin arrays will be produced from solid rectangular bar with dimensions 180x120x20 mm. The fins will be as integral part with the base-plate. The fin configurations, having fin length of 180 mm, will be tested at Set-up. For all fin configurations, the base-plate thickness and the width of the fin array were kept fixed at 5 mm and 120 mm respectively. The dimensions of the fin configurations are listed in Table 1. The geometry of the fin arrays is illustrated in Figure 5.

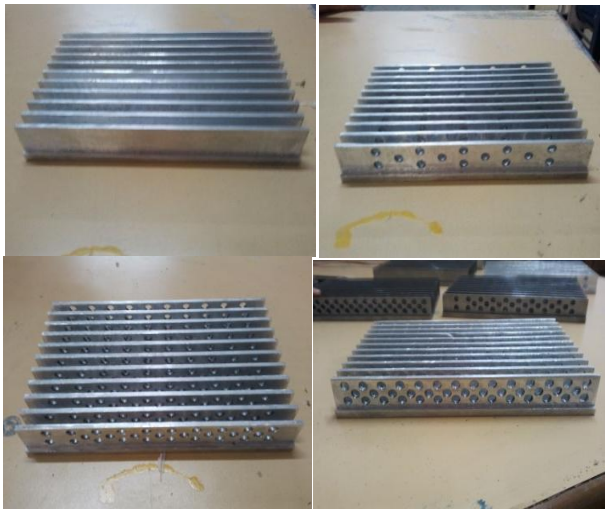

Figure 5. All Fin Geometry

During the experiments, both electrical power measurements and temperature measurements will be performed in order to supply desired power inputs to the heaters and read the ambient temperature and the temperature values at various locations on the fin base-plates. The electrical power will be supplied through a

IARJSET
ISSN (Online) 2393-8021
ISSN (Print) 2394-1588
International Advanced Research Journal in Science, Engineering and Technology
ISO 3297:2007 Certified
Vol. 3, Issue 9, September 2016

regulated a-c supply. The output of supply will be fed to two variable transformers so that for each of the set-ups, the power inputs could be selected independently. The ambient temperature will be measured by using mercury in glass thermometer with accuracy. The base-plate temperatures of fin arrays will be measured at six points by K type thermocouples. The measurements will be done at six points in order to see if large variations exist along the base-plate. The average of these six readings was taken as the plate temperature. To avoid disturbing the flow past the front surface, temperature measurements were not made at the fin tips. Since fin material (aluminum) has high thermal conductivity and fin heights are short (maximum fin height is 20mm), it was assumed that the temperatures along the fin and at the fin tip did not vary significantly from the base-plate.

After calibrating the experimental set-ups and verifying the calibration method, fin arrays will be mounted into the cases of Set-up. For each of the fin arrays, the power input will be adjusted to 25 W initially and the base-plate will be heated for about 10 hours. Then, the base temperature will be measured by means of six thermocouples located on the outer surface of base plate. In order to decide whether the fin array is at steady-state or not, the thermocouple readings will be taken at thirty minute intervals and this condition was assumed to be reached when the difference between two successive readings of each thermocouple is less than 0.5ºC. The base-plate temperature Tw, the ambient temperature Ta and the power input to the heater Q will be recorded at steady-state. The testing procedure mentioned above will be repeated for the power inputs25W, 33 W, 42 W, 52 W and 67.5 W for all the fin arrays. The calibration equations, will then employed to evaluate the total heat transfer rates from the fin arrays.

3. ANALYSIS

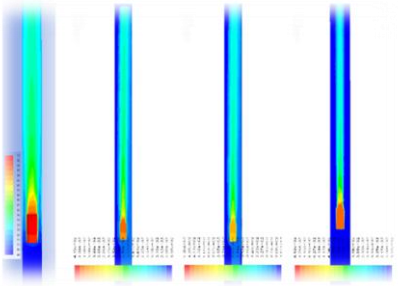

Figure 6 Static temperatute profile

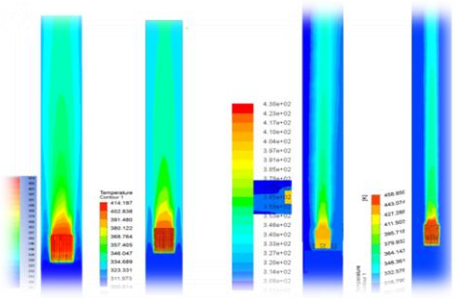

Figure 7 Temperature Contour

4. FLOW VISULIZATION

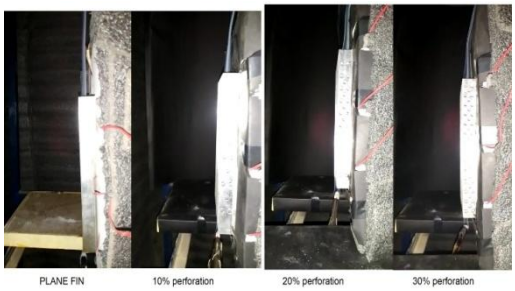

Figure 8 Chimney flow when smoke filament place near to tip

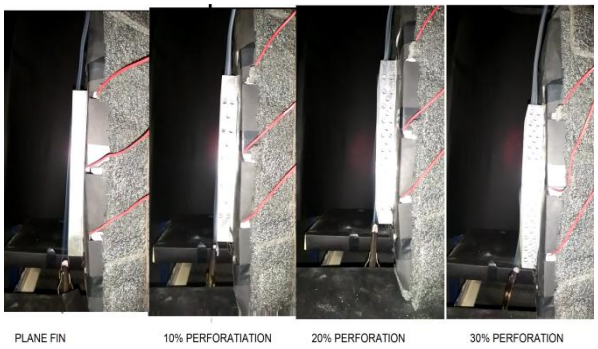

Figure 9 Chimney flow when smoke filament place away from tip

Above figure shows the chimney flow pattern of fin arrays that indicate that percentage of perforation affected the flow of chimney. We found that smoke placed at tip we observe plane fin have poor chimney flow pattern and percentage of perforation increase with increase the flow pattern near to base surface hence increase the heat transfer rate of fin with moving towards the base plate. Second figure indicate that we placed smoke away from tip then also developed the pattern of chimney flow. We increase the distance between the tip and smoke filament then we observe that 30 % perforation have maximum distance to developed the flow

5. RESULTS AND DISCUSSION

The overall heat transfer rates from fin arrays and the vertical flat plate are plotted as a function of base-to-ambient temperature difference for 10%, 20%, 30% perforation

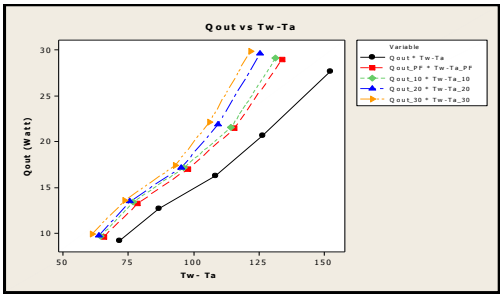

Figures 10 Variation of Total Heat Transfer with Base-to-Ambient Temperature Difference

IARJSET
ISSN (Online) 2393-8021
ISSN (Print) 2394-1588
International Advanced Research Journal in Science, Engineering and Technology
ISO 3297:2007 Certified
Vol. 3, Issue 9, September 2016

As observed in Figures 10, the total heat transfer rate from fin arrays depends on base-to-ambient temperature difference and percentage of perforation. As this temperature difference increases, total heat transfer increases. For the same base-to-ambient temperature difference, total heat transfer is Minimum for vertical flat plate while it increases for plane finned surface and goes on increasing as percentage of perforation increases. The total heat transfer is Maximum for 30% perforated fin array as shown in above fig. From these heat transfer rates radiation heat transfer is subtracted to obtain the convective heat transfer.

The radiation heat transfer rates from fin arrays and the vertical flat plate are plotted as a function of base-to-ambient temperature difference for 10%, 20%, 30%perforation.

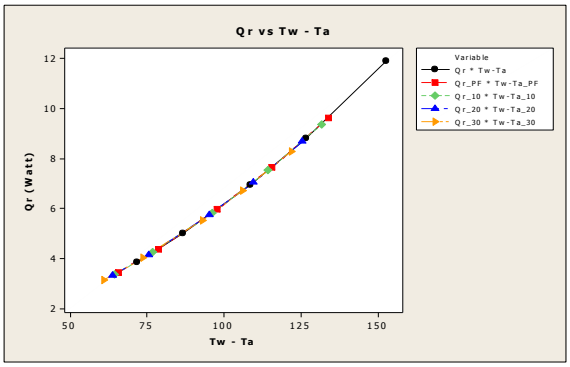

Figures 11 Variation of Radiation Heat Transfer Rate with Base-to-Ambient Temperature Difference

As observed in Figures 11, the radiation heat transfer peaks at the top of the fin where it has maximum base to ambient temperature difference and it receives more radiation from it. As the radiation heat transfer decreases with decreasing the base to ambient temperature difference, there is more available surface for radiation exchange which is the reason for increase in values of radiation heat flux. Therefore vertical plate has maximum radiation than other fin array. The convection heat transfer rates from fin arrays and the vertical flat plate are plotted as a function of base-to-ambient temperature difference for 10%, 20%, 30% perforation.

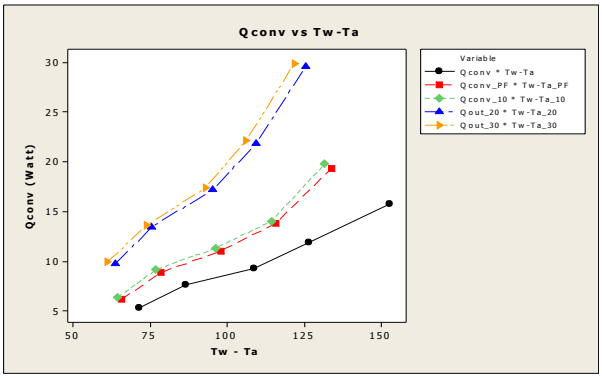

Figures 12 Variation of Convection Heat Transfer Rate with Base-to-Ambient Temperature Difference

As observed in Figures 12, the convection heat transfer rate from fin arrays depends on base-to-ambient temperature difference and percentage of perforation. As this temperature difference increases, convection heat transfer increases. For the same base-to-ambient temperature difference, convective heat transfer is Minimum for vertical flat plate while it increases for plane finned surface and goes on increasing as percentage of perforation increases. The convection heat transfer is Maximum for 30% perforated fin array as shown in above fig.

REFERENCES

[01] Starner K.E. and McManus H.N., "An Experimental Investigation of Free Convection Heat Transfer from Rectangular Fin Arrays", Journal of Heat Transfer, 273-278, (1963)
[02] Leung C.W. and Probert S.D., "Thermal Effectiveness of Short-Protrusion Rectangular, Heat-Exchanger Fins", Applied Energy, 1-8, (1989)
[03] Leung C.W., et al., "Heat transfer performances of vertical rectangular fins protruding from rectangular base : effect of fin length", Applied Energy, 313-318, (1986)
[04] Welling J.R. and Wooldridge C.N., "Free Convection Heat Transfer Coefficients from Vertical Fins", Journal of Heat Transfer, 439-444, (1965)
[05] Leung C.W. and Probert S.D., "Heat-Exchanger Design: Optimal Uniform Thickness of Vertical Rectangular Fins Protruding Perpendicularly Outwards, at Uniform Separations, from a Vertical Rectangular 'Base'", Applied Energy, 111-118, (1987)
[06] Yüncü H. and Anbar G., "An Experimental Investigation on Performance of Rectangular Fins on a Horizontal Base in Free Convection Heat Transfer", Heat and Mass Transfer, 507-514, (1998)
[07] Xiaoling Yu , Jianmei Feng, Quanke Feng, Qiuwang Wang, "Development of a Plate-Pin Fin Heat Sink and its Performance Comparisons with a Plate Fin Heat Sink", Applied Thermal Engineering 25, 2005, pp.173–182.
[08] Raaid R. Jassem, "Effect the form of Perforation on the Heat Transfer in the Perforated Fins" Academic Research International, volume 4, number 3, May 2013, pp.198-207..
[09] Kavita H. Dhanawade, Vivek K. Sunnapwar and Hanamant S. Dhanawade, "Thermal Analysis of Square and Circular Perforated Fin Arrays by Forced Convection", International Journal of Current Engineering and Technology, 2014.
[10] Md.FarhadIsmail,MuhammadNomanHasan,SuvashC.saha"Numeric al study of turbulent fluid flow and heat transfer in lareral perforated extended surfaces". Energy 4 (2014) 632- 639.
[11] Rigan Jain and M.M.Sahu., "Comparative Study of performances of Trapezoidal and Rectangular fins on a Vertical base under free convection heat transfer" IJERT vol.2 (2013) 261-272
[12] Amer Al-Damook, N. Kapur, J.L. Summers, H.M. hompson, "An experimental and computation investigation of thermal air flows through perforated pin heat sink", Elsevier Applied Thermal Engineering 89 (2015) 365-376
[13] Mohamad I. Al-Widyan, Amjad Al-Shaarawi, "Numerical Investigation of Heat Transfer Enhancement for a Perforated Fin in Natural Convection" IJERA, Vol. 2, Issue 1, Jan-Feb 2012, pp.175-184.
[14] Abdullah H. AlEssa et.al. "Enhancement of natural convection heat transfer from a fin by rectangular perforations with aspect ratio of two" International Journal of Physical Sciences Vol. 4 (10), pp. 540-547, October, 2009
[15] Incropera F.P. and DeWitt D.P., Fundamentals of Heat and Mass Transfer, John Wiley & Sons, New York, (1990)
[16] McAdams W. H., Heat Transmission, McGraw-Hill, New York, (1954)
[17] Bejan A., Convection Heat Transfer, John Wiley & Sons, New York, (1984)